European Heart Journal (2009) **30**, 2861–2868
doi:10.1093/eurheartj/ehp322

In vivo myocardial distribution of multipotent progenitor cells following intracoronary delivery in a swine model of myocardial infarction

Hung Q. Ly[1,4]*, Kozo Hoshino[1], Irina Pomerantseva[3,1], Yoshiaki Kawase[1], Ryuichi Yoneyama[1], Yoshiaki Takewa[1], Annik Fortier[4], Summer L. Gibbs-Strauss[2], Carrie Vooght[2], John V. Frangioni[2], and Roger J. Hajjar[1]

[1]Mount Sinai School of Medicine, New York, NY, USA; [2]Beth Israel Deaconess Medical Center, Harvard Medical School, Boston, MA, USA; [3]Massuchetts General Hospital, Harvard Medical School, Boston, MA, USA; and [4]Department of Medicine, Montreal Heart Institute, Université de Montréal, 5000 Belanger Street (east), Montréal, QC, Canada

Received 21 July 2008; revised 16 June 2009; accepted 24 July 2009; online publish-ahead-of-print 17 August 2009

Aims There are few data comparing the fate of multipotent progenitor cells (MPCs) used in cardiac cell therapy after myocardial infarction (MI). To document *in vivo* distribution of MPCs delivered by intracoronary (IC) injection.

Methods and results Using an anterior MI swine model, near-infrared (NIR) fluorescence was used for *in vivo* tracking of labelled MPCs [mesenchymal stromal (MSCs), bone marrow mononuclear (BMMNCs), and peripheral blood mononuclear (PBMNCs)] cells early after IC injection. Signal intensity ratios (SIRs) of injected over non-injected (reference) zones were used to report NIR fluorescence emission. Following IC injection, significant differences in mean SIR were documented when MSCs were compared with BMMNCs [1.28 ± 0.10 vs. 0.77 ± 0.11, $P < 0.001$; 95% CI (0.219, 0.805), respectively] or PBMNCs [1.28 ± 0.10 vs. 0.80 ± 0.14, $P = 0.005$; 95% CI (0.148, 0.813), respectively]. Differences were maintained during the 60 min tracking period, with only the MSC-injected groups continuously emitting NIR fluorescence (SIR$>$1). This is correlated with greater cell retention for MSCs relative to mononuclear cells. However, there was evidence of MSC-related vessel plugging in some swine.

Conclusion Our *in vivo* NIR fluorescence findings suggest that MPC distribution and retention immediately after intracoronary delivery vary depending on cell population and could potentially impact the clinical efficacy of cardiac cell therapy.

Keywords *In vivo* • Multipotent progenitor cells • Intracoronary • Myocardial infarction • Near-infrared fluorescence

Introduction

Cell-based therapy for myocardial repair has recently garnered a great deal of interest, emerging as a promising adjunctive therapy for ischaemic heart disease.[1–3] A growing body of evidence has alluded to its beneficial role in the setting of myocardial infarction (MI).[4,5] A rapid transition towards clinical application has lead to cautious optimism but has prompted a call for further translational research using clinically relevant large animal models to clarify the contributions of multipotent progenitor cells (MPCs).[5,6] As such, tracking the biological fate of these cells remains a pivotal issue. Near-infrared (NIR) fluorescence imaging, an established *in vivo* molecular imaging modality, could be used to track transplanted MPCs.[7,8] Cell retention after intracoronary (IC) injection may be altered not only due to the injured cardiac milieu, but also because MPCs vary in their ability to home and engraft to the latter. Thus, we hypothesize that, in the immediate phase after IC delivery, the *in vivo* myocardial distribution and retention in infarcted myocardium will differ depending on the MPC population.

Methods

Intracoronary delivery of MPCs was compared in the setting of infarcted myocardium. A total of 15 swine were included in the study; three expired at the time of MI model creation. Of the remainder, 12 swine

* Corresponding author. Tel: +1 514 376 3330, Fax: +1 514 376 6299, Email: hung.ly@icm-mhi.org

were equally divided into three study groups: mesenchymal stem cells (MSCs), bone marrow mononuclear cells (BMMNCs), and peripheral blood mononuclear cells (PBMNCs). Every third swine was assigned, in a non-randomized fashion, to a specific cell injection group. A decision was made a priori to limit this study to 15 swine for budgeting reasons. Institutional committees on research animal care approved the study protocol. All study animals received humane care in accordance with the Principles of Laboratory Animal Care (National Society of Medical Research) and the Guide for the Care and Use of Laboratory Animals (Institute of Laboratory Animal Resources and the National Institutes of Health).

Isolation of multipotent progenitor cell populations

The collection and isolation methods were chosen to best reflect those used in prior clinical studies of cardiac cell therapy.[9–11] Please refer to Supplementary material online, *Methods* for techniques used to harvest PBMNCs, BMMNCs, and MSCs.

Myocardial infarction creation and intracoronary cell delivery

Myocardial infarction was created by a 60 min balloon occlusion of the proximal left anterior descending artery (LAD) (Supplementary material online). Study animals were brought back on day 3–4 post-MI for cell injection.

In each study group, a total of 2.0×10^7 cells were labelled with 1–2 μM IR-786 perchlorate (Sigma) diluted in serum-free DMEM, with an incubation time of 20 min at 37°C and 5% CO_2[12] (*Figure 1A* and *B*). IR-786-loaded cells were examined under NIR fluorescence microscopy to ensure successful labelling. For injection, all labelled cells were washed twice with PBS then suspended in a final injection volume of 5 mL of sterile PBS. An over-the-wire balloon catheter system was used for cell delivery and, relying on recorded images during MI creation, the first diagonal in each swine was used as a landmark to position the delivery catheter system. Subsequently, cells were slowly injected (over 3 min) after transient balloon occlusion. Following *in vivo* MPC tracking, IC administration of cardioplegic solution (Plegisol, Hospira Inc., IL, USA) was used to perform humane euthanasia and hearts were harvested for analyses.

Calibration of near-infrared signal intensity and cell number

To correlate the number of cells retained after delivery and the emitted NIR signal, NIR phantoms were used and calibration curves were constructed as previously described.[13] Briefly, IR-786 loaded MPCs were suspended in a 1 cm path length cuvette at a concentration of 5×10^3 cells/μL. For our purpose, our correlation studies were performed with only MSCs and mononuclear cells isolated from BM, as PBMNCs represent a more lineage-driven, circulating cell population from BMMNCs. Absorbance spectrometry was performed using a HR2000 fibre optic spectrometer and a DH2000-BAL light source (Ocean Optics, Florida). Emitted fluorescence was measured

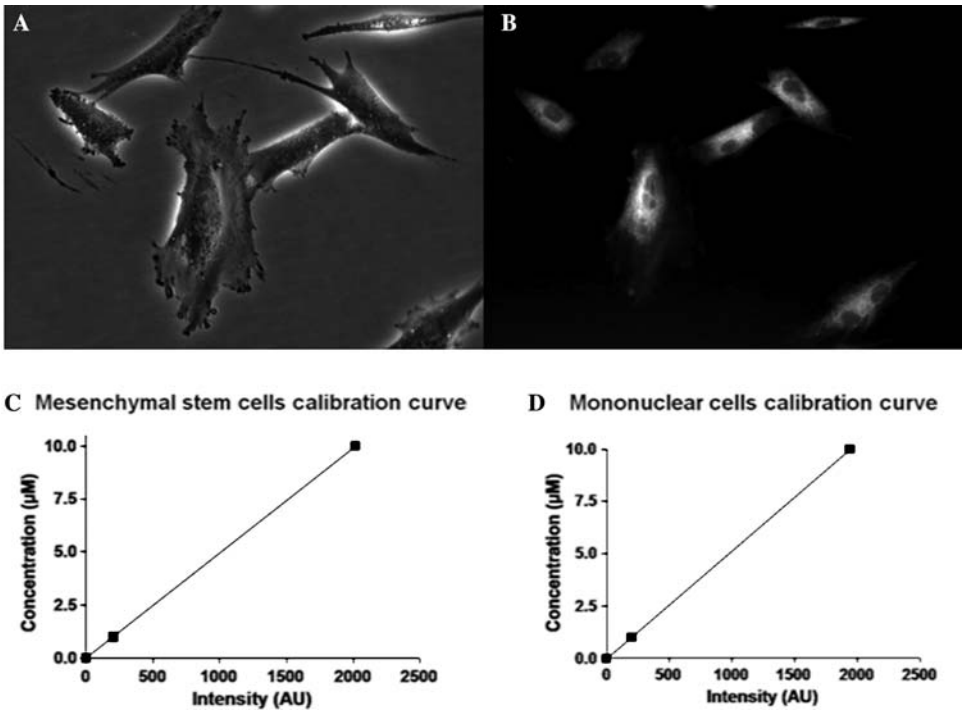

Figure 1 (*A–D*) IR-786 loading of multipotent progenitor cells and cell calibration curves. BMMNC, PBMNC, and MSC were labelled with the NIR fluorophore, IR-786 perchlorate. After a 20 min incubation period, MPCs incorporated the imaging probe intracellularly, which renders them trackable with the high-sensitivity fluorescence system (see text for details). Shown are *ex vivo* expanded, early passage MSC after IR-786 loading (A: phase image; B: NIR image). Calibration curves [for MSC (*C*) and mononuclear cells (*D*)] were constructed after absorbance spectrometry was performed on labelled cells suspended in a 1 cm path length cuvette. The measured NIR SI could then be translated to absolute cell number (expressed as equivalence of ICG) (see text).

after excitation with a NIR light source with defined wavelengths, fluence rates, and exposure times. With the latter parameters held constant, the ratio of MPC-related signal intensity (SI) to background could then be translated to absolute cell number. The quantified NIR emissions of each MPC population were subsequently expressed as 'indocyanine green (ICG) equivalence' (*Figure 1C* and *D*).[13] Such a measure of equivalence will standardize the fluorescence emitted by different MPC populations and, consequently, permits their comparison.

In vivo near-infrared imaging and fluorescence signal intensity analysis

For post-injection tracking, *in vivo* open-chest imaging was performed after conventional midline sternotomy to suspend the heart in a pericardial cradle and centre the anterior wall of the left ventricle within the imaging field. The *in vivo* imaging system has been previously described.[14] Briefly, the system is self-contained and mobile thus can be readily positioned over the surgical field for optimal imaging. Separate or merged colour video and fluorescence images are obtained by way of a dichroic mirror, which splits emitted light into visible or NIR light. Every 100 ms, real-time simultaneous anatomic (colour) and functional (NIR fluorescence) imaging data are captured by the respective cameras. Subsequently, measurement of fluorescence SI was done off-line. Quantification of SI was obtained by an operator-determined circumscribed region of interest, which provides SI statistics such as mean, maximum and minimum for the selected area. Assessors who performed imaging analyses were blinded to cell injection group assignments.

Emitted SIs from the myocardial surface were deemed of adequate intensity if documented above background signal noise. Mean SIs were measured at the base (Zone 1; above the first diagonal artery), the mid-LV (Zone 2; between the first diagonal and the terminal bifurcation of the LAD), and the apex (Zone 3; beyond the terminal bifurcation of the LAD) (*Figure 2*). Serial measurements were made at the following time points: 1 min prior to cell delivery, at 2, 5, 10, 15, 30, 45, and 60 min after injection.

For each time point, a signal intensity ratio (SIR) was calculated (*Figure 2*). For all computations, as balloon occlusion and MPC injection were performed beyond the first diagonal artery, the base of the heart (Zone 1) was used as the reference zone, whereas the mid-segment and the apex were considered part of the infarcted territory. The SIR was obtained by dividing the mean SI from an infarcted zone by the mean SI from the reference zone, at each time point of the tracking period.

Normalizing the emitted SI using the SIR therefore allows for comparisons between IR-786 labelled MPC groups, as uptake of the fluorophore (and subsequent emitted SIs) may vary according to cell size.

Statistical analyses

Continuous variables were reported as mean $\pm$ standard error. In order to assess how the SIR change over time, a linear growth model with two covariates (cells, zone) was adjusted using the SAS procedure PROC MIXED. CELLS and ZONE effect were included in a CLASS statement with an ID variable to identify the subject of analysis. Time from injection was considered as a continuum and included in a RANDOM statement, just like the ZONE term and an intercept term. A full model with all the interaction terms (CELLS|ZONE|TIME) was adjusted. In the case of significant interaction, contrasts were used to compare cells groups. All tests were two-sided and a *P*-value less than 0.05 was considered significant. Analyses were performed with SAS (v.9.1.3; SAS Institute Inc., NC, USA).

Results

All MPC groups were labelled with the NIR fluorophore IR-786 as described and, by Trypan Blue exclusion test, cell viability for all cell groups was >90% prior to injection. IR-786 loaded cells were found to exhibit NIR fluorescence corresponding to 8.9 and 5.7 attomole equivalents of ICG per MSC and mononuclear cells, respectively.

Following injection after recent infarction, significant differences in mean SIR were documented when MSCs were compared with BMMNCs [1.28 ± 0.10 vs. 0.77 ± 0.11, $P < 0.001$; 95% CI (0.219, 0.805), respectively] or PBMNCs [1.28 ± 0.10 vs. 0.80 ± 0.14, $P = 0.005$; 95% CI (0.148, 0.813), respectively] (*Figure 3A*).

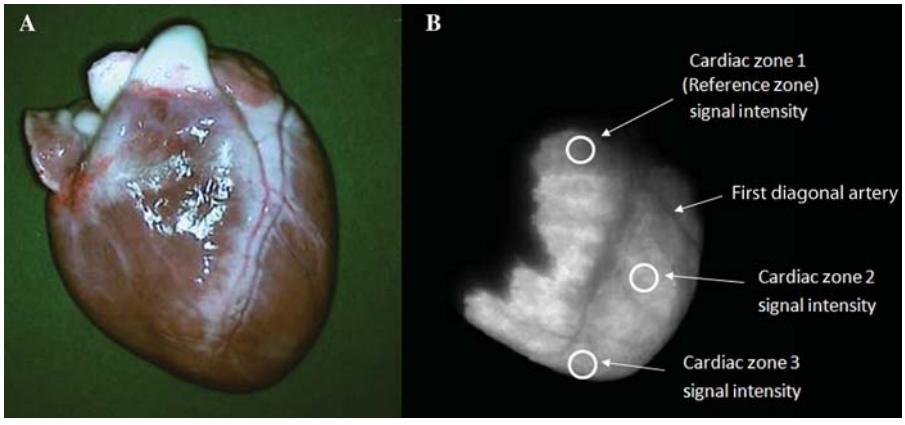

Figure 2 Near-infrared signal intensity analysis and the signal intensity ratio. The SIR was obtained by dividing the mean SI from a cardiac zone by the mean SI from the reference zone. Since MPC injection occurred at the level of the first diagonal artery, the base of the heart was used as the reference zone, whereas the mid-segment and the apex were (injected) cardiac Zones 2 and 3, respectively. Shown as example is an explanted, uninjured heart after BMMNC delivery (*A*: colour image; *B*: NIR image).

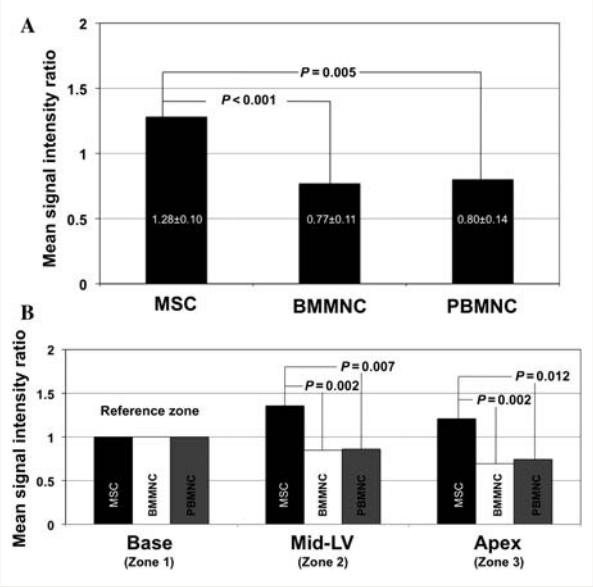

Figure 3 Mean signal intensity ratios of multipotent progenitor cell populations after intracoronary injection in infarcted hearts. (*A*) Change in mean signal intensities by cell population: when compared with hearts injected with MSCs, *in vivo* tracking of those injected with labelled-BMMNCs and PBMNCs found to less emitted NIR fluorescence, corresponding to mean SIR less than one; (*B*) Signal intensity ratios according to cardiac zones: MPCs were compared according to infarcted cardiac zones, with significant differences in mean SIRs documented between cell groups. Using the non-injected, uninjured zone (base of the heart) as a reference, only MSCs exhibited SIRs greater than one in injected zones (mid-segment and apex).

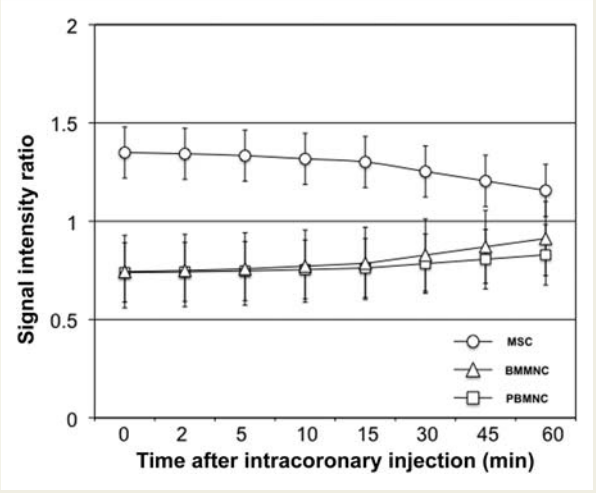

Figure 4 Signal intensity ratio changes over time in injured myocardium. Over the 60 min cell tracking period after intracoronary injection, MSCs, BMMNCs, and PBMNCs displayed different *in vivo* retention. Despite declines in mean SIRs over time, MSC-injected hearts were consistently documented with SIR more than one. Conversely, signal intensities emitted from transplanted BMMNC or PBMNC were never recorded with SIR greater than one. Such a finding is consistent with lesser retention of the latter MPCs in the injected cardiac zones. $P = 0.005$.

This contrast between MSCs and BMMNCs or MSCs and PBMNCs remained unchanged when MPCs were compared over either the mid- or apical segments (cardiac Zones 2 and 3, respectively) (*Figure 3B*). Differences between MPCs were maintained over time. While decreases in emitted NIR during *in vivo* tracking occurred for BMMNCs and PBMNCs, MSCs always maintained SIR >1 (*Figure 4*).

After IC injection, MPC myocardial distribution closely followed the vascular territory of the LAD (*Figure 5A–C*). During *in vivo* monitoring of the anterior wall, with the exception of infarct zones, MPCs appear to distribute homogenously as there were no significant differences in NIR emitted between cardiac Zones 2 and 3 for MSC (mean SIR 1.36 ± 0.11 vs. 1.21 ± 0.11; $P = 0.07$, 95% CI $(-0.01, 0.31)$], BMMNC (mean SIR 0.85 ± 0.12 vs. 0.69 ± 0.12; $P = 0.10$, 95% CI $(-0.03, 0.34)$], and PBMMNC (mean SIR 0.86 ± 0.15 vs. 0.74 ± 0.15; $P = 0.302$, 95% CI $(-0.107, 0.341)$]. When examining explanted heart sections, the full thickness of the myocardium was found to be NIR-emitting, thus IR-786 loaded MPCs circulated from the epicardial artery to the microcirculation. However, we also confirmed that MPCs did not permeate scarred areas distribution, likely due to post-infarction microvascular bed injury (*Figure 5D*). By NIR fluorescence microscopy, NIR-emitting cells could be documented in sections taken only from border and infarct zones of myocardial tissue with very few labelled cells found in the healthy myocardium. The documented progressive decline in SI after injection correlated with declining numbers of retained cell in injured hearts, in both peri-infarct and infarct zones (*Figure 6A–C*).

Finally, during *in vivo* MSC tracking, vessel plugging was documented after injection into injured hearts. This did not occur immediately upon cell bolus injection as there was no abrupt cessation of antegrade flow nor was there acute ST-elevation on continuous monitoring as would be expected if embolization occurred during the course of injection. Further, no study animals expired abruptly. Vessel plugging was observed to occur progressively well beyond the first pass and upon recirculation of injected MPCs during the 60 min period of *in vivo* tracking (*Figure 7*). This occurred in three swine. This phenomenon was not documented in the mononuclear cell populations.

Discussion

Recent trials have reported on the benefits of cell-based therapy as an adjunctive therapy in acute MI.[15–17] Nevertheless, these findings have been contradicted by findings of equivocal clinical efficacy on cardiac function and structure.[18,19] Hence, such contrasting clinical data have prompted a call for further translational research using clinically relevant large animal models with a focus on mechanistic questions in order to push the field forward.[3,20] At the moment, with IC injection into the infarct-related artery being arguably the most widely used route of delivery, there are limited data comparing the myocardial distribution of different MPCs. Our study extends on these findings by providing *in vivo* data tracking and comparing different MPC populations and how they interact with

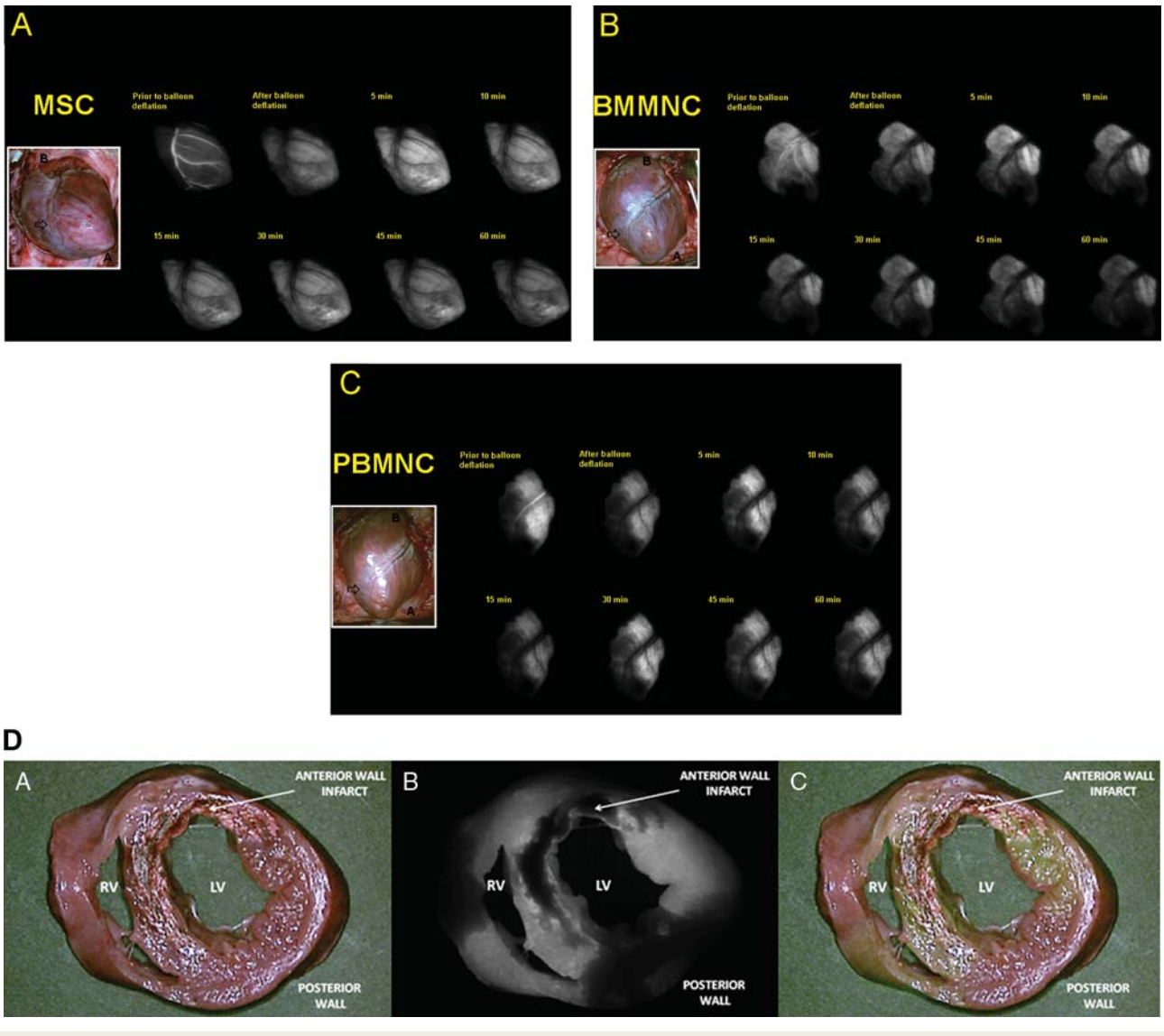

Figure 5 Myocardial distribution of multipotent progenitor cells following intracoronary delivery. Near-infrared imaging data are captured at various tracking time points immediately after intracoronary delivery of MSCs (*A*), BMMNCs (*B*), and PBMNCs (*C*) in the setting of recent infarction. Multipotent progenitor cells readily distribute along the vascular territory of the infarct-related artery. Cell boluses are seen to occupy the intravascular space (top left panel in each figure) and then permeate myocardial tissue after balloon deflation. Shown inset is a colour image of the infarcted heart (B: base; A: apex; Infarct: anterior wall infarct zone); (*D*) Once injected by intracoronary route, MPCs were documented to penetrate the vascular territory perfused by the left anterior descending artery, in effect permeating the full thickness of the cardiac muscle. In this 'bread loaf' section of an infarcted heart after MSC injection, only the scarred area did not show evidence of NIR emission. (*A*: colour image; *B*: NIR image; *C*: merge image; INF: infarct zone; RV: right ventricle; LV: left ventricle).

the infarcted microenvironment in the immediate phase after IC injection.

Near-infrared fluorescence imaging has emerged as a promising imaging modality for *in vivo* tracking of transplanted cells, making use of either organic (e.g. green fluorescence protein, polymethines) or organic/hybrid (quantum dots) exogenous contrast agents.[7,21] Near-infrared fluorophores (such as IR-786) have high photon absorption and lower tissue scatter than visible wavelengths. In addition, this optical molecular imaging modality is well-suited for conventional microscopy permitting pathological specimen to be scrutinized at the single-cell level.[12,22] Near-infrared fluorescence offers high sensitivity, provides tomographic imaging capabilities and there is no evidence at present that dye released from dead/dying cells is accumulated by macrophages, a common problem with iron-based MRI contrast agents. Two drawbacks to bear in mind with NIR fluorescence tracking are its fundamental limitation with regard to depth of tissue penetration (1–5 mm for reflectance imaging; 1–4 cm for tomographic imaging) and the dilution of the NIR fluorophore with cell division.[23,24] The present study lasted 60 min in duration and, as previously

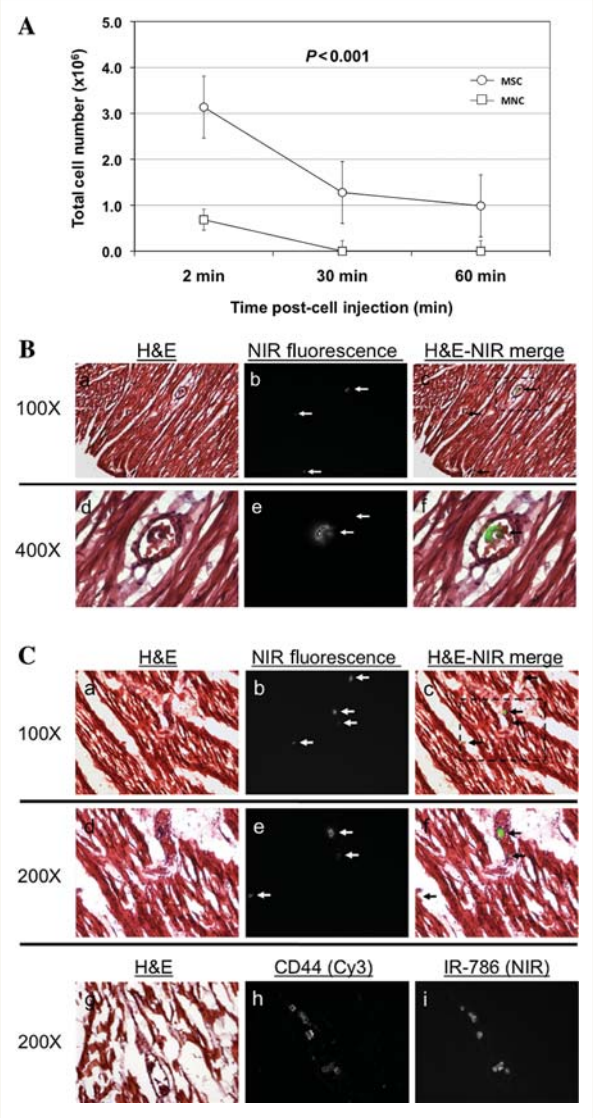

Figure 6 Cell loss and poor multipotent progenitor cell retention over time after intracoronary injection. (*A*) Although all MPC groups showed a rapid decline in signal intensity, a lack of discernable SI relative to background was documented in mononuclear cell populations. This finding correlated with poor myocardial cell retention in infarcted tissue. This was not the case for injected MSC. In addition, MPC cell loading with IR-786 allowed for the examination of injected tissue with NIR fluorescence microscopy. Shown are standard Haematoxylin & Eosin histological sections taken from the (*B*) border zone and (*C*) infarct zone from an infarcted heart after MSC injection (A+D: H & E; B+E: NIR images; C+F: merged images). Despite detection at the single cell level being possible, only a few MSCs were detected at 60 min after cell delivery (white arrow, $b + c$ and $e + f$). After intracoronary injection into the infarct-related artery, treatment of histological sections with a CD44 primary antibody and Cy3 secondary antibody revealed plasma membrane staining in >95% of cells showing cytoplasmic NIR fluorescence from IR-786 (lower row, G+H+I].

reported by our group, IR-786 is stable for hours *in vivo*.[25] In addition, MPCs were washed thoroughly before injection making the likelihood of dye leakage negligible.

One of the best-characterized NIR fluorophores is ICG, which has a quantum yield of 13% in dimethylsulfoxide and similar absorption and emission peaks as IR-786. As discussed previously, reporting IR-786 NIR fluorescence intensity as equivalents of ICG fluorescence permits comparison of findings.[13] In our study, IR-786 loaded MSCs and mononuclear cells exhibited NIR fluorescence equivalent to 8.9 and 5.7 attomole equivalents of ICG per MSC and BM cell, respectively. Thus, NIR fluorophore uptake correlated with cell size and their brightness seen during imaging. Given these values, the high resolution of our NIR fluorescence imaging system, and the low NIR autofluorescence of heart,[13] it is likely therefore that relatively small numbers of stem cells were detectable *in vivo* immediately following IC delivery.

Engraftment of delivered MPC remains a daunting challenge, especially in the setting of a hostile, inflammatory microenvironment. There is evidence that the ischaemic myocardial microenvironment is not only conducive but essential in MPC engraftment.[26,27] Our findings highlight that the injured cardiac milieu alters *in vivo* MPC retention differently with mononuclear cells rapidly declining or disappearing after injection. Although the phenomenon of recirculation of injected cells could arguably lead to progressively greater cell numbers being ultimately retained in cardiac tissue, there was no re-increase in SI during our 60 min tracking period. In addition, the likelihood of recirculation contributing to greater retention remains low as most mononuclear cells will home to or remain trapped in organs such as the spleen or liver.[28] Moreover, as reported recently by Doyle *et al.*[29], differences in retention according to IC injection technique (by single bolus technique vs. by stop-flow technique) are not significant and will likely not overcome the important washout effect after balloon deflation. Thus, our findings corroborate prior reports from both animal and human studies reporting poor cell retention following MPC delivery in infarcted microenvironment (on the order of 1.3–17.8% of injected cells).[28–30]

The appropriateness and safety of IC administration of MSC remains disputed. Investigators have reported on the clinical safety and feasibility of MSC IC injection in MI patients.[9,11] Conversely, Vulliet *et al.*[31] reported on the acute embolization of microvessels following IC delivery of MSC, whereas Freyman *et al.*[32] documented only transient decreased coronary blood flow (without evidence of microinfarction) combined to greater MSCs engraftment and an improvement in efficacy after IC injection. Alternatively, Perin *et al.*[33] recently provided crucial information in a pilot study on the safety of IC delivery of MSCs. It would seem that the issue is not so much the route of administration as it is the rate at which the cell bolus is delivered. Rates of cell administration greater than 1.5×10^6/min were associated with an incremental rise in biomarkers of cardiac injury.[33]

Our inconsistent finding of vessel plugging (not all MSC-injected swine had evidence of distal embolization) points to additional mechanisms of IC-injected MSC for improved retention. Though simple physical characteristics of MPCs (cell size or microvascular

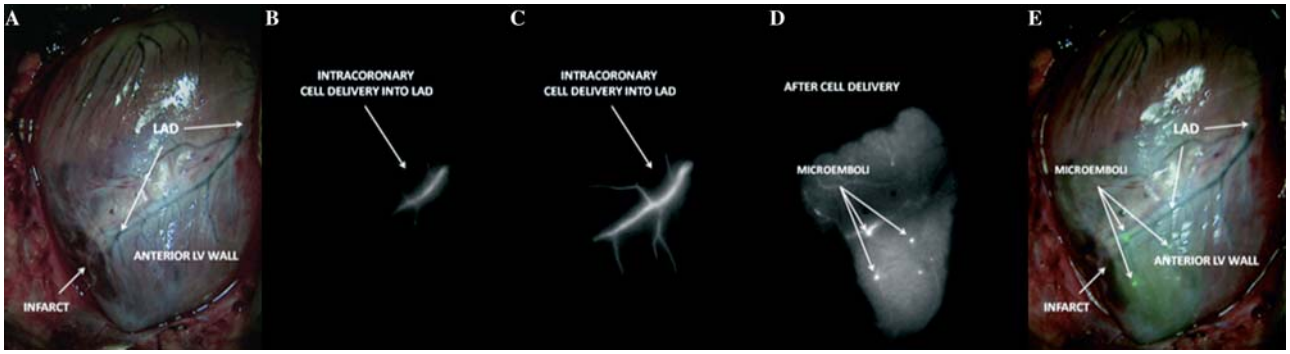

Figure 7 Evidence of progressive vessel plugging after MSC delivery during *in vivo* cell tracking after intracoronary delivery. Although no abrupt arrest of antegrade flow was documented at the time of cell injection, intracoronary delivery of MSC was followed by vessel plugging (*A*: colour image; *B*: NIR image at start of intracoronary injection; *C*: NIR image during intracoronary injection without evidence of abrupt flow arrest; *D*: NIR image taken at 20 min post-injection; *E*: merge image of NIR image with emboli and colour image) (LAD: left anterior descending artery).

obstruction) are plausible, one should also consider the contribution of biological processes related to cellular trafficking, i.e. the ability of IC-delivered MPC to home to, adhere to and transmigrate through injured endothelium into the cardiac microenvironment.[34,35] While speculative, our findings point to the possibility that inflammation following MI could potentiate greater adhesion between circulating or injected MSCs (once exposed to the *in vivo* milieu) and lead to their progressive cellular impaction and clumping in myocardial vessels. Enhanced MSC adhesion to cardiac microvascular endothelium has been previously described due to the inflammatory state elicited by an acute MI, resulting from greater VCAM-1 expression mediating the cellular interaction.[34] Nevertheless, due to the potential for detrimental effects of acute microinfarction and/or progressive vascular plugging, the IC injection of MSCs in the post-MI setting remains controversial and caution should be exercised when considering this specific route of delivery.

Key limitations of our study need to be considered. *In vivo* tracking was limited to the early phase (the first pass and the subsequent 60 min) after IC injection. Multipotent progenitor cells were unfractionated and more selected populations [for example, CD34+, CD133+, or MAPCs (multipotent adult progenitor cells)] could have interacted differently with injured myocardium. Only one rate of cell infusion was investigated and cell injection was done on day 3–4 post-MI. Another time window for IC delivery could potentially favour greater cell engraftment. Moreover, other investigators have shown that intramyocardial or transvenous cell delivery might prove more efficacious, we only focused on the IC route.[30] Assessment of MI size was not performed, and along with the inherent variations in coronary anatomy between study animals, could act as important confounders in the observed differences in MPC myocardial distribution and retention. Finally, NIR image guidance was used to select samples of myocardium with a high cell fraction and frozen sectioning of saturated cardiac tissue specimens exhibiting retention of full NIR fluorescence. However, after standard histological processing, we realized that a majority of IR-786 (a lipophilic fluorophore) was removed. It was later found that tissue processing required alternative fixation using methods to preserve IR-786 in labelled cells (further detailed in Supplementary material online).

In conclusion, our study provides both *in vivo* evidence of the poor myocardial retention (in the immediate, early phase after IC delivery) of MPCs as well as *in vivo* proof of a potential deleterious effect of the IC delivery of MSC when administered after recent MI, i.e. vessel plugging through cell impaction and clumping. These findings highlight important efficacy and safety issues to consider for future clinical trials.

Supplementary material

Supplementary material is available at *European Heart Journal* online.

Funding

This study was supported by grants from the National Institutes of Health: R01-CA-115296 (J.V.F.) and R01 HL078691, HL057263, HL071763, HL080498, and HL083156, and a Leducq Transatlantic Network (R.J.H.).

Conflict of interest: none declared.

References

1. Ott HC, McCue J, Taylor DA. Cell-based cardiovascular repair—the hurdles and the opportunities. *Basic Res Cardiol* 2005;**100**:504–517.
2. Boyle AJ, Schulman SP, Hare JM, Oettgen P. Controversies in cardiovascular medicine: ready for the next step. *Circulation* 2006;**114**:339–352.
3. Wollert KC, Drexler H. Clinical applications of stem cells for the heart. *Circ Res* 2005;**96**:151–163.
4. Wollert KC, Drexler H. Cell therapy for acute myocardial infarction: where are we heading? *Nat Clin Pract Cardiovasc Med* 2004;**1**:61.
5. Murry CE, Field LJ, Menasche P. Cell-based cardiac repair: reflections at the 10-year point. *Circulation* 2005;**112**:3174–3183.
6. Welt FG, Losordo DW. Cell therapy for acute myocardial infarction: curb your enthusiasm? *Circulation* 2006;**113**:1272–1274.
7. Frangioni JV. *In vivo* near-infrared fluorescence imaging. *Curr Opin Chem Biol* 2003;**7**:626–634.

8. Bengel FM, Schachinger V, Dimmeler S. Cell-based therapies and imaging in cardiology. *Eur J Nucl Med Mol Imaging* 2005;**32**(Suppl. 2):S404–S416.
9. Chen SL, Fang WW, Ye F, Liu YH, Qian J, Shan SJ, Zhang JJ, Chunhua RZ, Liao LM, Lin S, Sun JP. Effect on left ventricular function of intracoronary transplantation of autologous bone marrow mesenchymal stem cell in patients with acute myocardial infarction. *Am J Cardiol* 2004;**94**:92–95.
10. Assmus B, Schachinger V, Teupe C, Britten M, Lehmann R, Dobert N, Grunwald F, Aicher A, Urbich C, Martin H, Hoelzer D, Dimmeler S, Zeiher AM. Transplantation of Progenitor Cells and Regeneration Enhancement in Acute Myocardial Infarction (TOPCARE-AMI). *Circulation* 2002;**106**: 3009–3017.
11. Katritsis DG, Sotiropoulou PA, Karvouni E, Karabinos I, Korovesis S, Perez SA, Voridis EM, Papamichail M. Transcoronary transplantation of autologous mesenchymal stem cells and endothelial progenitors into infarcted human myocardium. *Catheter Cardiovasc Interv* 2005;**65**:321–329.
12. Nakayama A, Bianco AC, Zhang CY, Lowell BB, Frangioni JV. Quantitation of brown adipose tissue perfusion in transgenic mice using near-infrared fluorescence imaging. *Mol Imaging* 2003;**2**:37–49.
13. De Grand AM, Lomnes SJ, Lee DS, Pietrzykowski M, Ohnishi S, Morgan TG, Gogbashian A, Laurence RG, Frangioni JV. Tissue-like phantoms for near-infrared fluorescence imaging system assessment and the training of surgeons. *J Biomed Opt* 2006;**11**:014007.
14. De Grand AM, Frangioni JV. An operational near-infrared fluorescence imaging system prototype for large animal surgery. *Technol Cancer Res Treat* 2003;**2**: 553–562.
15. Assmus B, Honold J, Schachinger V, Britten MB, Fischer-Rasokat U, Lehmann R, Teupe C, Pistorius K, Martin H, Abolmaali ND, Tonn T, Dimmeler S, Zeiher AM. Transcoronary transplantation of progenitor cells after myocardial infarction. *N Engl J Med* 2006;**355**:1222–1232.
16. Schachinger V, Erbs S, Elsasser A, Haberbosch W, Hambrecht R, Holschermann H, Yu J, Corti R, Mathey DG, Hamm CW, Suselbeck T, Assmus B, Tonn T, Dimmeler S, Zeiher AM. Intracoronary bone marrow-derived progenitor cells in acute myocardial infarction. *N Engl J Med* 2006;**355**: 1210–1221.
17. Schachinger V, Erbs S, Elsasser A, Haberbosch W, Hambrecht R, Holschermann H, Yu J, Corti R, Mathey DG, Hamm CW, Suselbeck T, Werner N, Haase J, Neuzner J, Germing A, Mark B, Assmus B, Tonn T, Dimmeler S, Zeiher AM. Improved clinical outcome after intracoronary administration of bone-marrow-derived progenitor cells in acute myocardial infarction: final 1-year results of the REPAIR-AMI trial. *Eur Heart J* 2006;**23**:2775–2783.
18. Lunde K, Solheim S, Forfang K, Arnesen H, Brinch L, Bjornerheim R, Ragnarsson A, Egeland T, Endresen K, Ilebekk A, Mangschau A, Aakhus S. Anterior myocardial infarction with acute percutaneous coronary intervention and intracoronary injection of autologous mononuclear bone marrow cells: safety, clinical outcome, and serial changes in left ventricular function during 12-months' follow-up. *J Am Coll Cardiol* 2008;**51**:674–676.
19. Janssens S, Dubois C, Bogaert J, Theunissen K, Deroose C, Desmet W, Kalantzi M, Herbots L, Sinnaeve P, Dens J, Maertens J, Rademakers F, Dymarkowski S, Gheysens O, Van Cleemput J, Bormans G, Nuyts J, Belmans A, Mortelmans L, Boogaerts M, Van de Werf F. Autologous bone marrow-derived stem-cell transfer in patients with ST-segment elevation myocardial infarction: double-blind, randomised controlled trial. *Lancet* 2006;**367**:113–121.
20. Rosenzweig A. Cardiac cell therapy—mixed results from mixed cells. *N Engl J Med* 2006;**355**:1274–1277.
21. Frangioni JV, Hajjar RJ. *In vivo* tracking of stem cells for clinical trials in cardiovascular disease. *Circulation* 2004;**110**:3378–3383.
22. Zaheer A, Lenkinski RE, Mahmood A, Jones AG, Cantley LC, Frangioni JV. *In vivo* near-infrared fluorescence imaging of osteoblastic activity. *Nat Biotechnol* 2001;**19**: 1148–1154.
23. Ntziachristos V, Bremer C, Weissleder R. Fluorescence imaging with near-infrared light: new technological advances that enable *in vivo* molecular imaging. *Eur Radiol* 2003;**13**:195–208.
24. Sevick-Muraca EM, Houston JP, Gurfinkel M. Fluorescence-enhanced, near infrared diagnostic imaging with contrast agents. *Curr Opin Chem Biol* 2002;**6**:642–650.
25. Flaumenhaft R, Tanaka E, Graham GJ, De Grand AM, Laurence RG, Hoshino K, Hajjar RJ, Frangioni JV. Localization and quantification of platelet-rich thrombi in large blood vessels with near-infrared fluorescence imaging. *Circulation* 2007; **115**:84–93.
26. Frangogiannis NG, Smith CW, Entman ML. The inflammatory response in myocardial infarction. *Cardiovasc Res* 2002;**53**:31–47.
27. Vandervelde S, van Luyn MJ, Tio RA, Harmsen MC. Signaling factors in stem cell-mediated repair of infarcted myocardium. *J Mol Cell Cardiol* 2005;**39**:363–376.
28. Hofmann M, Wollert KC, Meyer GP, Menke A, Arseniev L, Hertenstein B, Ganser A, Knapp WH, Drexler H. Monitoring of bone marrow cell homing into the infarcted human myocardium. *Circulation* 2005;**111**:2198–2202.
29. Doyle B, Kemp BJ, Chareonthaitawee P, Reed C, Schmeckpeper J, Sorajja P, Russell S, Araoz P, Riederer SJ, Caplice NM. Dynamic tracking during intracoronary injection of 18F-FDG-labeled progenitor cell therapy for acute myocardial infarction. *J Nucl Med* 2007;**48**:1708–1714.
30. Hou D, Youssef EA, Brinton TJ, Zhang P, Rogers P, Price ET, Yeung AC, Johnstone BH, Yock PG, March KL. Radiolabeled cell distribution after intramyocardial, intracoronary, and interstitial retrograde coronary venous delivery: implications for current clinical trials. *Circulation* 2005;**112**(Suppl. 9):I150–I156.
31. Vulliet PR, Greeley M, Halloran SM, MacDonald KA, Kittleson MD. Intra-coronary arterial injection of mesenchymal stromal cells and microinfarction in dogs. *Lancet* 2004;**363**:783–784.
32. Freyman T, Polin G, Osman H, Crary J, Lu M, Cheng L, Palasis M, Wilensky RL. A quantitative, randomized study evaluating three methods of mesenchymal stem cell delivery following myocardial infarction. *Eur Heart J* 2006;**27**:1114–1122.
33. Perin EC, Silva GV, Assad JA, Vela D, Buja LM, Sousa AL, Litovsky S, Lin J, Vaughn WK, Coulter S, Fernandes MR, Willerson JT. Comparison of intracoronary and transendocardial delivery of allogeneic mesenchymal cells in a canine model of acute myocardial infarction. *J Mol Cell Cardiol* 2008;**44**:486–495.
34. Segers VF, Van Riet I, Andries LJ, Lemmens K, Demolder MJ, De Becker AJ, Kockx MM, De Keulenaer GW. Mesenchymal stem cell adhesion to cardiac microvascular endothelium: activators and mechanisms. *Am J Physiol Heart Circ Physiol* 2006;**290**:H1370–H1377.
35. Ceradini DJ, Gurtner GC. Homing to hypoxia: HIF-1 as a mediator of progenitor cell recruitment to injured tissue. *Trends Cardiovasc Med* 2005;**15**:57–63.